

ENGINEERING AND GINNING

Charting the Collision Between a Seed Coat Fragment and Newly Designed Lint Cleaner Grid Bars

Carlos B. Armijo*, Derek P. Whitelock, Sidney E. Hughs, Edward M. Barnes, and Marvis N. Gillum

ABSTRACT

An experiment was conducted to determine how a seed coat fragment (SCF) reacts after colliding with each of 10 different experimental grid bars mounted on a saw-type lint cleaner simulator. A high-speed video camera recorded the action that took place. The included angle of the sharp toe of the grid bars (or the clockwise angle from vertical) ranged from 30° to 105° in 15° increments. A rounded grid bar with a 0.76-mm (0.030-in) radius was also included in the experiment. Results showed that grid bars that had an included angle of the toe of the grid bar larger than the included angle found on conventional grid bars appeared to adequately remove a SCF. Also, grid bars that had a second corner a short distance from the toe of the grid bar appeared to remove the SCF more quickly and completely from the fiber bundle, and after separation from the fiber bundle, the SCF retained more energy and its momentum continued for a longer time period. Considering the position of the SCF a short time (700 µs) after impact with the grid bar, grid bars that had a 105°, 60°, and 45° included angle from the toe of the grid bar, and the rounded grid bar, performed best in removing SCFs from fiber bundles. These grid bars warrant further testing on a full-size conventional lint cleaner.

Seed coat fragments (SCFs) are a known issue for the textile industry and methods that create less or remove SCFs during the harvesting or ginning process is an on-going focus of research at the USDA-ARS Southwestern Cotton Ginning Research Laboratory. This research uses a cultivar known to have a seed coat that breaks easily and contaminates

ginned lint with SCFs. Recent research has attempted to remove SCFs at the harvester, saw gin stand, roller gin stand, and seed-cotton cleaning process. Armijo et al. (2006a) found that auxiliary rib guides on the saw gin stand did not reduce the number of Advanced Fiber Information System (AFIS) seed coat neps. The most recent studies have used AFIS seed coat neps as an indicator of the presence of SCFs. In the same study by Armijo et al. (2006a), it was found that roller ginning did not reduce AFIS seed coat nep count. In another study, Armijo et al. (2006b) found that seed coat nep counts might be reduced by using a small diameter spindle on the picker harvester or by ginning on a powered roll gin stand. The powered roll gin stand used a paddle to assist turning the seed roll in the gin stand. Spinning tests on fiber from the study by Armijo et al. (2006b) have not yet been completed to substantiate the reduction in seed coat neps. Another study by Armijo et al. (2009a) found that seed coat nep counts were not reduced by different levels of seed-cotton cleaning with inclined cylinder cleaners and stick machines.

Past studies by Mangialardi and Shepherd (1968) and Mangialardi (1987) showed that SCFs were not reduced with different levels of saw-type lint cleaning. Both of these studies used conventional grid bars in the lint cleaners. Leonard et al. (1982) tested notched grid bars on a saw-type lint cleaner, and found that even though the notched grid bars reduced lint cleaner waste and lint loss, fiber quality was not improved and the grid bars were not recommended over conventional grid bars. Baker and Brashears (1989) tested grid bar spacing, grid sharpness, and grid-to-saw clearance, and found that grid bar spacing and sharpness affected lint loss but did not improve fiber quality. The studies by Leonard et al. (1982) and Baker and Brashears (1989) did not focus on removing SCFs. More recently, there has been related research on grid bar designs by Whitelock and Anthony (2003), Ray (2006), and Wanjura et al. (2009), but these studies evaluated grid bars on machines used mainly to clean seed cotton, and not lint, and they also did not focus on removing SCFs. Armijo et al. (2008) summarized past research that used photographic techniques to

C.B. Armijo, D.P. Whitelock, S.E. Hughs, and M.N. Gillum, USDA-ARS Southwestern Cotton Ginning Research Laboratory, PO Box 578, Mesilla Park, NM 88047; E.M. Barnes, Cotton Incorporated, 6399 Weston Parkway, Cary, NC 27513

*Corresponding author: cararmij@nmsu.edu

study the path that fibers take as they are drawn over a lint cleaner grid bar, and described preliminary work that used a high-speed video camera to examine a fiber bundle with an attached SCF colliding with model-sized experimental grid bars mounted on a lint cleaner simulator. The most recent research continues this theme of modeling the removal of SCFs using a saw-type lint cleaner simulator. The objective of this study was to evaluate how an SCF reacts after colliding with newly-designed grid bars mounted on a lint cleaner simulator using a high-speed video camera.

MATERIALS AND METHODS

Figure 1 shows the lint cleaner simulator and digital high-speed video camera used in the study performed at the USDA-ARS Southwestern Cotton Ginning Research Laboratory located in Mesilla Park, NM. The lint cleaner simulator incorporates a 0.41-m (16-in) diameter, 6.4-mm (0.250-in) thick disk that represented the lint cleaner saw. The disk rotated at 1,000 rpm (a tangential velocity of 21.6 m/s or 4,250 ft/min). A 1.1 kW (1.5 hp) variable-speed motor powered the disk. A 1.6-mm (0.063-in) diameter, 3.2-mm (0.125-in) long tube representing a saw tooth was attached to the periphery of the disk. A fiber bundle containing one SCF was threaded into the tube such that the distance between the tube and the center of the SCF was approximately 3 mm (0.118 in). The distance between the tube and the grid bar was approximately 1 mm (0.039 in). A solenoid moved the grid bar into position to collide with the SCF at the same instant the video camera was activated.

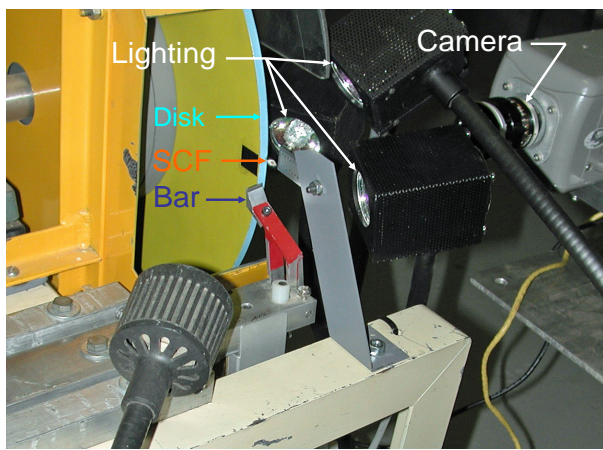


Figure 1. Lint cleaner simulator and high-speed video camera.

The high-speed camera was a Phantom V7.1 (Vision Research, Wayne, NJ) with a 50-mm lens and 10-mm extension tube. The video camera was set to record at 10,000 frames per second. This recording rate allowed a 512 x 384 pixel resolution. The exposure time on the camera was set at 2 μ s. The camera had 14,509 frames of memory in which to capture the collision of the SCF and grid bar. The movement of the tube holding the SCF between each frame was 2.16 mm (0.085 in) and the time between each frame was 100 μ s. The camera had a 4800 ISO/ASA monochrome sensitivity, which reduced the lighting requirements. Lighting consisted of three 250 W high-intensity tungsten halogen lamps located 57 to 90 mm (2.2-3.5 in) away from the disk.

Figure 2 shows the designs of the 10 experimental grid bars used in the test. Grid bar designs included bars with a single corner or edge, a double edge, a groove following an edge, no edge at all (rounded), and varying angles that the edge made from vertical. The included angle of the sharp toe of the grid bars (or the clockwise angle from vertical) ranged from 30° to 105° in 15° increments. The 105°, 90°, 75°, and 60° grid bars had a small surface of about 1.5 mm (0.059 in) from the toe of the bar, giving these bars a second edge to possibly help remove the SCF. The 90° L grid bar ("L" denotes L-shape) had a surface of 4 mm (0.157 in) from the toe of the bar, also giving this bar a second corner. The 60° G and 45° G grid bars ("G" denotes groove) had a 0.51-mm (0.020-in) deep groove on the surface of the bar about 1.5 mm (0.059 in) from the toe of the bar, the idea being that the groove would act similar to a second edge where the SCF would drop into the groove upon impact and be removed more easily. The 45° and 30° grid bars did not have a second edge; the surface length from the toe of the grid bar on these bars was approximately 10 mm (0.394 in) and 15 mm (0.591 in), respectively. The 0° R grid bar ("R" denotes rounded) did not have an edge at all, but instead had a 0.76 mm (0.030 in) radius. A conventional lint cleaner grid bar typically has an included angle of the sharp toe of about 30° on the first grid bar, and about 55° on the remaining bars, but none of the conventional grid bars have a second corner. The 60° and 30° experimental grid bars were essentially the same design as conventional grid bars.

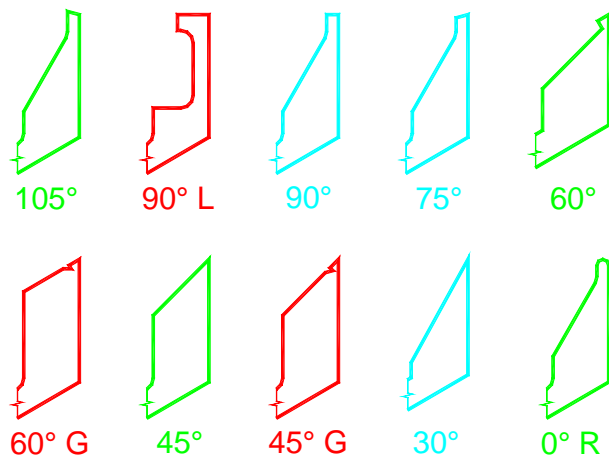


Figure 2. Cross section of experimental grid bars.

The test consisted of the 10 experimental grid bars, two types of cotton, and three replications for a total of 60 lots. The cottons included a common upland cultivar that does not have a history of excessive SCF formation and a cultivar known to have a fragile seed coat. Both cultivars were grown in the Mesilla Valley of southern New Mexico. The fiber bundle/SCF samples were weighed before and after impact in a controlled environmental room set at a temperature of 21°C (70°F) and relative humidity of 65%. The experimental design was a randomized complete block with replications serving as blocks. Analysis of variance was performed with the General Linear Model of SAS (version 9.1; SAS Institute, Inc., Cary, NC) and differences between main effect treatment means were tested with Tukey's studentized range test.

RESULTS AND DISCUSSION

Figures 3 through 12 show the path of the center of the SCF (hereafter, “center of the SCF” will be referred to as SCF) before and after impact with each of the 10 experimental grid bars shown in Fig. 2. (Refer to Armijo et al. (2009b) to see a short video sequence of an SCF colliding with each of the experimental grid bars.) Because statistics showed that cultivar was not different among grid bar designs, the two cultivars were combined and the positions of the SCF shown in Figs. 3 through 12 were the average of six lots (two cultivars and three replications). The elapsed time between each point shown in Figs. 3 through 12 was constant at 100 µs (one video frame). The distance between each point was a graphical representation of velocity with respect to each 100 µs interval; the larger the distance between points, the greater the velocity.

The reference point (RP) shown in Figs. 3 through 12 was the position of the SCF immediately before impact with the leading edge of the grid bar (the edge closest to the tube). The RP was used to verify that the SCF was oriented similarly in the tube before interaction with the grid bar for each run and as a starting point to determine how far and in what direction the SCF traveled after impact with the grid bar. The point 100 µs before RP was used to calculate velocity of the SCF attached to the disk. Figures 3 through 12 also show the position of the SCF when it collided with the experimental grid bars (designated CP for collision point), and the position of the SCF 700 µs, or seven video frames after the SCF impacted the grid bar (designated “700 µs” in the figures).

Tables 1, 2, and 3 show the position and velocity of the SCF at RP, at CP, and 700 µs after collision, respectively, for each of the grid bars. The x and y coordinates in the tables are in relation to the leading edge of the grid bar. A negative x-coordinate value signifies position or travel of the SCF to the left of the leading edge of the grid bar (away from the disk). A positive x-coordinate value signifies position or travel of the SCF to the right of the leading edge of the grid bar (towards the disk). A negative y-coordinate value signifies position or travel of the SCF below the leading edge of the grid bar (downward from the grid bar), and a positive y-coordinate value signifies position or travel of the SCF above the leading edge of the grid bar (upwards from the grid bar). An ideal situation would be for the grid bar to cause the SCF to be removed, and then travel in a mostly horizontal direction away from the disk (negative x-coordinate value) where the SCF would not be re-entrained with the fiber bundle attached to the disk. The data in Tables 1 through 3, as well as observations made of the videos are included in later discussions about Figs. 3 through 12.

Table 1 shows that at RP, the position of the SCF in both the x- and y-direction was not different among grid bars. This was by design and confirms that the fiber bundle/SCF specimen was loaded into the tube at about the same position every time. At RP for all of the grid bars, the SCF was positioned approximately 1 mm (0.039 in) above the leading edge of the grid bars (positive y-direction) and approximately -3 mm (-0.118 in) to the left of the leading edge of the grid bars (negative x-direction). Although the position of the SCF in the x-direction

was not different among grid bars at RP, a covariant analysis showed that the position of the SCF at RP was directly related to the position of the SCF at 700 µs after collision (Observed Significance Level = 0.0053). In other words, as the initial position (RP) of the SCF in the x-direction moved closer to the disk, the less likely it was that the SCF was ginned. Because the results of the covariant analysis were similar to the results in Table 3 (700 µs after collision), covariant analysis was not included. The original weight of the fiber bundle/SCF ranged from 4 to 10 mg (0.06 to 0.15 grains) and was not significantly different among grid bars. At RP, the velocity of the SCF in the x-direction was not different among grid bars and averaged -0.91 m/s (-2.99 ft/s). The velocity of the SCF in the y-direction was different among grid bars, the main difference being that the 90° L grid bar was -17.9 m/s (-58.7 ft/s, downward direction) and the other nine grid bars averaged -21.5 m/s (-70.5 ft/s), about the same velocity as the disk (21.6 m/s or 70.9 ft/s). Acceleration of the SCF was highly variable and did not indicate any consistent trends in the tests (data not shown).

Table 1. Means and statistical analyses of position and velocity of the SCF at the reference point immediately before impact with the grid bars (RP in Figs. 3 through 12). The x and y coordinates are in relation to the leading edge of the grid bar.

Grid Bar	Immediately before collision			
	Position, mm		Velocity, m/s	
	x	y	x	y ^z
105°	-3.25	1.28	-0.57	-21.65 b
90° L	-2.37	1.54	-1.20	-17.94 a
90°	-3.13	1.10	-0.43	-21.94 b
75°	-3.36	0.58	-0.71	-21.37 b
60°	-3.22	1.10	-0.86	-21.51 b
60° G	-3.11	0.91	-2.28	-21.51 b
45°	-3.05	0.53	-1.29	-21.37 b
45° G	-2.72	0.94	-0.43	-21.66 b
30°	-2.79	1.57	-0.86	-21.08 ab
0° R	-3.02	0.50	-0.43	-21.08 ab
Observed Significance Level ^y				
NS	NS	NS	0.0362	

^z Means followed by the same letter in each column are not different based on Tukey's studentized range test ($P \leq 0.05$).

^y NS = not statistically significant at $P > 0.05$.

Table 2. Means and statistical analyses of position and velocity of the SCF at the collision point with the grid bars (CP in Figs. 3 through 12). The x and y coordinates are in relation to the leading edge of the grid bar.

Grid Bar	At collision			
	Position, mm		Velocity, m/s	
	x	y ^z	x ^z	y ^z
105°	-3.06	-1.61 bc	2.57 ab	-10.54 abc
90° L	-2.17	1.06 a	2.05 abc	-4.78 ab
90°	-3.06	-1.79 bc	3.98 a	-10.54 abc
75°	-3.39	-1.47 bc	-0.29 abcd	-20.52 c
60°	-3.43	-2.29 c	-0.28 abcd	-12.25 abc
60° G	-3.40	-0.54 b	-2.99 bcd	-14.53 bc
45°	-3.48	-1.13 bc	-4.28 d	-16.53 c
45° G	-3.08	-0.97 bc	-3.56 cd	-19.09 c
30°	-2.95	-1.98 bc	-0.57 abcd	-14.67 bc
0° R	-3.04	-1.58 bc	0.14 abcd	-2.56 a
Observed Significance Level ^y				
NS	< 0.0001	0.0002	< 0.0001	

^z Means followed by the same letter in each column are not different based on Tukey's studentized range test ($P \leq 0.05$).

^y NS = not statistically significant at $P > 0.05$.

Figure 3 shows the result of the SCF colliding with the 105° grid bar. At CP, the fiber bundle was wrapped around both the leading and second edge of the grid bar, and pulled the SCF slightly back towards the grid bar just before the SCF made a clean break from the fiber bundle and became a free body. There was an appreciable drop in momentum (velocity) of the SCF after impact with the grid bar (the distance between the points decreased). The velocity of the SCF in the y-direction at impact decreased from -21.7 m/s (-71.2 ft/s, Table 1) to -10.5 m/s (-34.5 ft/s, Table 2). After impact with the grid bar, the SCF traveled in a mostly horizontal direction away from the disk, an ideal situation where the SCF was not re-trained with the fiber bundle attached to the disk. The velocity of the SCF in the x- and y-direction 700 µs after impact was -2.28 and 2.56 m/s (-7.48 and 8.40 ft/s, Table 3), respectively.

Figure 4 shows the results of the SCF colliding with the 90° L grid bar. The SCF impacted the top surface of the grid bar and then traveled back towards the disk. This was an undesirable situation where the SCF was not removed and continued on with the fiber bundle attached to the disk. At CP,

the velocity of the SCF in the y-direction decreased momentarily after impact with the grid bar from -17.9 m/s (-58.7 ft/s, Table 1) to -4.78 m/s (-15.7 ft/s, Table 2). The velocity of the SCF in the y-direction (still attached to the fiber bundle) 700 µs after impact was -16.7 m/s (-54.8 ft/s, Table 3), almost back to the original velocity of -17.9 m/s (-58.7 ft/s). The horizontal movement of the SCF after CP was due to the fibers in the bundle stretching and pulling on the SCF after impact with the grid bar. The 90° L grid bar did not work well mostly because the CP did not interact with the second edge of the grid bar, the second edge being too far away (4 mm or 0.157 in) to be of any benefit.

Figure 5 shows the results of the SCF colliding with the 90° grid bar. The distance between the leading edge and second edge of the 90° grid bar was 1.5 mm (0.059 in), considerably less than the 4 mm (0.157 in) of the 90° L grid bar. The second edge of the 90° grid bar helped to remove the SCF. At CP, the fiber bundle was wrapped around both the leading and second edge of the grid bar and pulled the SCF slightly back towards the grid bar (similar to action of the 105° grid bar). The velocity of the SCF in the y-direction at CP was reduced by about half from RP to -10.5 m/s (-34.4 ft/s, Table 2), also similar to the 105° grid bar. Immediately after the SCF made a clean break at CP, the SCF had little energy remaining and did not travel far from CP. The velocity of the SCF in the y-direction 700 µs after CP was reduced to -0.44 m/s (-1.44 ft/s, Table 3). Interestingly, high-speed videos showed that the angle of the fiber bundle with respect to the second edge of the 90° grid bar was similar to the angle observed with the 105° grid bar, but the results were different: at 700 µs after collision, the SCF was -2.51 mm (-0.099 in) further to the left (x-direction) of the leading edge of the 105° grid bar than with the 90° grid bar (Table 3).

Figure 6 shows the results of the SCF colliding with the 75° grid bar. At CP, the fiber bundle was wrapped around both the leading and second edge of the grid bar, and the SCF was pulled slightly back toward the disk similar to what occurred with the 105° and 90° grid bars. Shortly after CP the velocity of the SCF dropped considerably (the distance between the points decreased) as the SCF separated from the fiber bundle. The SCF lost all of its momentum 700 µs after CP; the velocity of the SCF in the x- and y-direction was 0.29 and 0.00 m/s (0.95 and 0.00 ft/s, Table 3), respectively, and the SCF had traveled back towards the grid bar.

Table 3. Means and statistical analyses of position and velocity of the SCF at 700 µs after collision with the grid bars (700 µs in Figs. 3 through 12). The x and y coordinates are in relation to the leading edge of the grid bar.

Grid Bar	700 µs after collision			
	x ^z	Y	x	y ^z
105°	-5.30 b	-1.13	-2.28	2.56 a
90° L	2.90 a	-4.68	-1.20	-16.74 b
90°	-2.79 ab	-1.54	2.14	-0.44 ab
75°	-2.28 ab	-1.05	0.29	0.00 ab
60°	-3.72 b	-0.56	-0.28	2.57 a
60° G	0.16 ab	-0.06	1.57	-1.14 ab
45°	-5.38 b	-1.73	-2.41	0.86 ab
45° G	0.04 ab	0.56	2.42	-2.14 ab
30°	-2.71 ab	-3.14	-3.27	-3.57 ab
0° R	-3.49 b	0.77	0.99	5.13 a
Observed Significance Level ^y				
	0.0005	NS	NS	0.0483

^z Means followed by the same letter in each column are not different based on Tukey's studentized range test ($P \leq 0.05$).

^y NS = not statistically significant at $P > 0.05$.

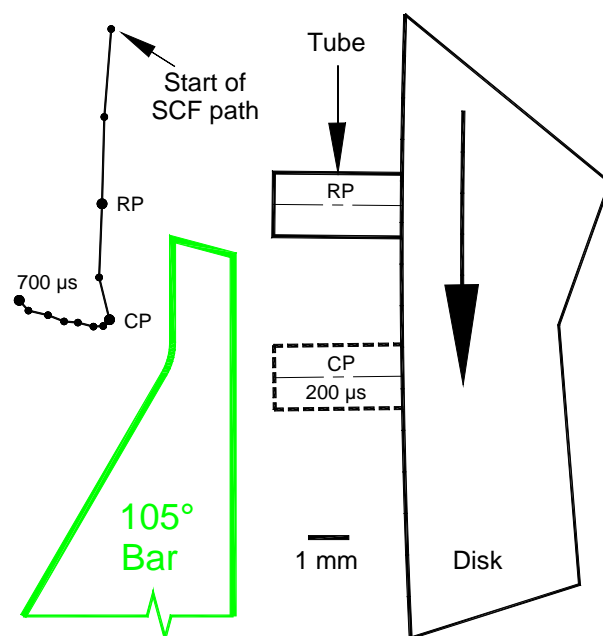


Figure 3. Grid bar: 105°. The distance from the toe to the 2nd corner is 1.55 mm (0.061 in). The SCF was removed on the second corner.

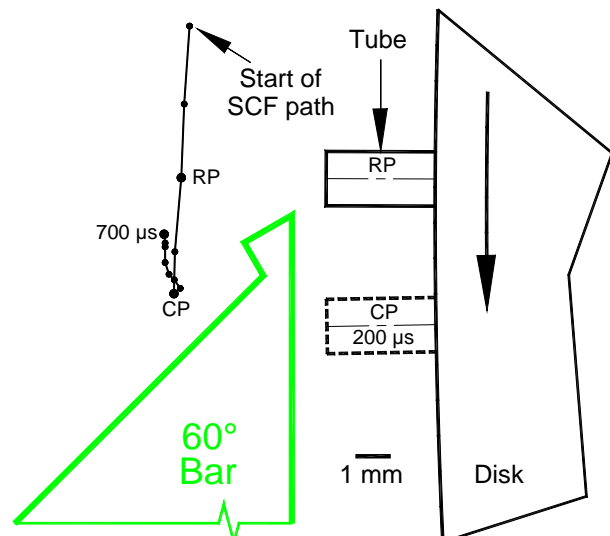
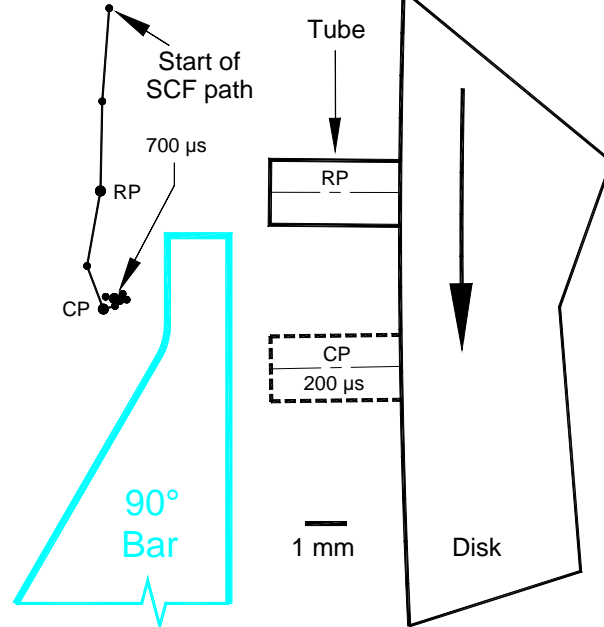
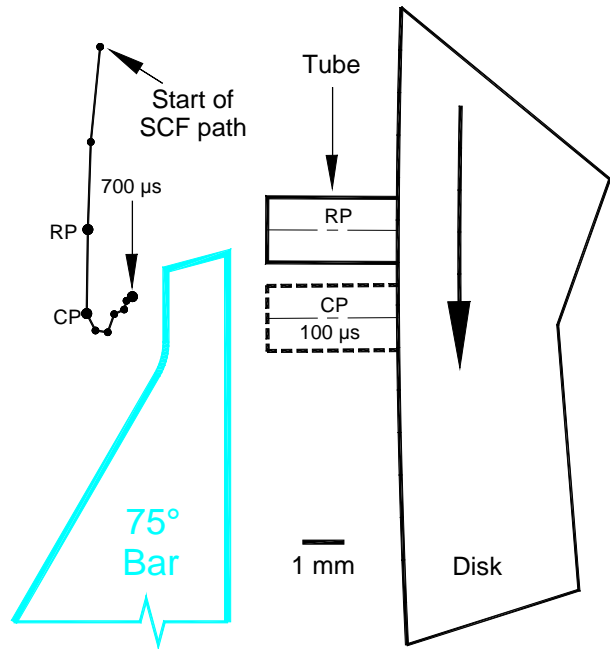
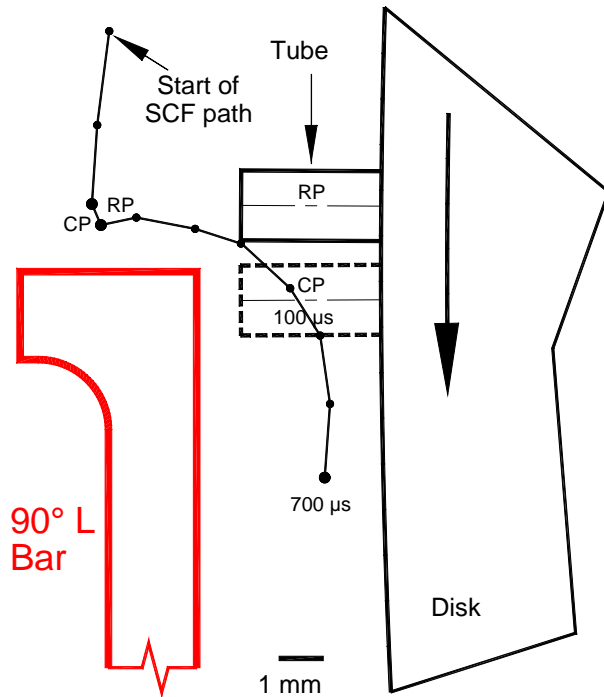


Figure 7 shows the results of the SCF colliding with the 60° grid bar. At CP, the fiber bundle was wrapped around both the leading and second edge of the grid bar, and the SCF was removed close to CP indicating that the fiber bundle did not greatly influence the removal of the SCF, but removal was mostly caused by the force of the SCF hitting the grid bar and making a clean break. At CP, the velocity of the SCF in the y-direction was -12.3 m/s (-40.4 ft/s, Table 2). After the SCF was removed from the fiber bundle, the SCF traveled in an upward direction away from the grid bar. The velocity of the SCF in the x- and y-direction 700 μs after collision was -0.28 and 2.57 m/s (-0.92 and 8.43 ft/s, Table 3), respectively.

ence the removal of the SCF, but removal was mostly caused by the force of the SCF hitting the grid bar and making a clean break. At CP, the velocity of the SCF in the y-direction was -12.3 m/s (-40.4 ft/s, Table 2). After the SCF was removed from the fiber bundle, the SCF traveled in an upward direction away from the grid bar. The velocity of the SCF in the x- and y-direction 700 μs after collision was -0.28 and 2.57 m/s (-0.92 and 8.43 ft/s, Table 3), respectively.

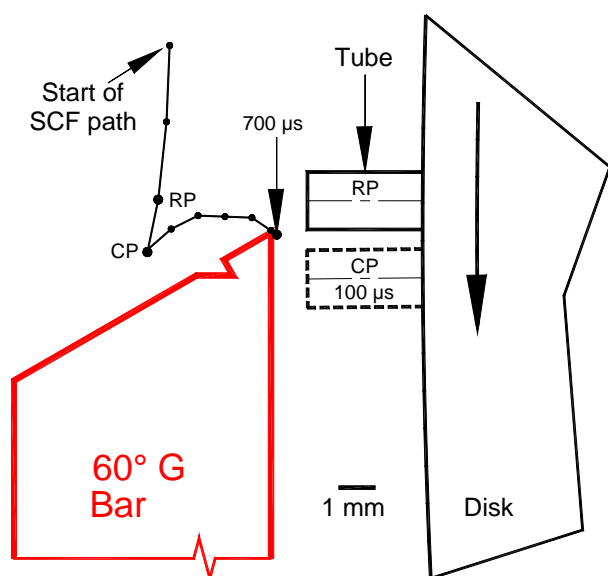


Figure 8. Grid bar: 60° G. The distance from the toe to the 2nd corner is 1.5 mm (0.059 in). The SCF was not removed.

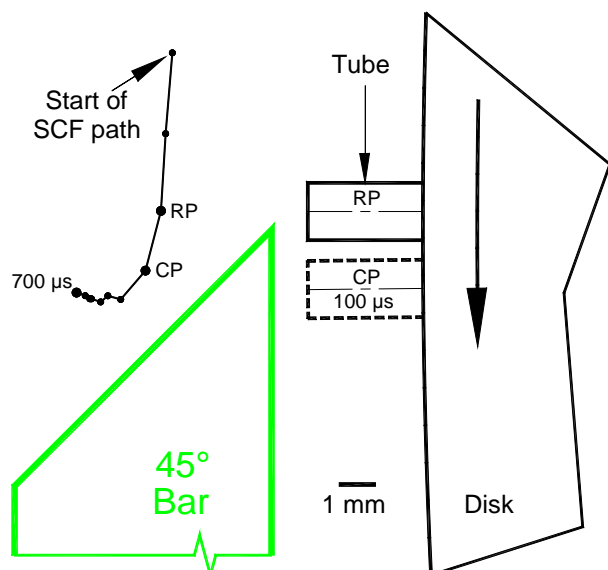


Figure 9. Grid bar: 45°. The distance from the toe to the 2nd corner is 10 mm (0.394 in). The SCF was removed at the toe of the grid bar.

Figure 8 shows the path of the SCF after colliding with the 60° G grid bar. The SCF impacted the grid bar but was not removed. The fiber bundle continued to pull the SCF back towards the disk as the bundle stretched around the leading edge of the grid bar. The groove did not function as a second edge to help remove the SCF because the groove was not large enough for the SCF to fit into. In addition, the groove may have cushioned the impact of the SCF. The velocity of the SCF in the x- and y-direction 700 μ s after impact was reduced to 1.57 and -1.14 m/s (5.15 and -3.74 ft/s, Table 3), respectively, and the SCF was located between the grid bar and disk.

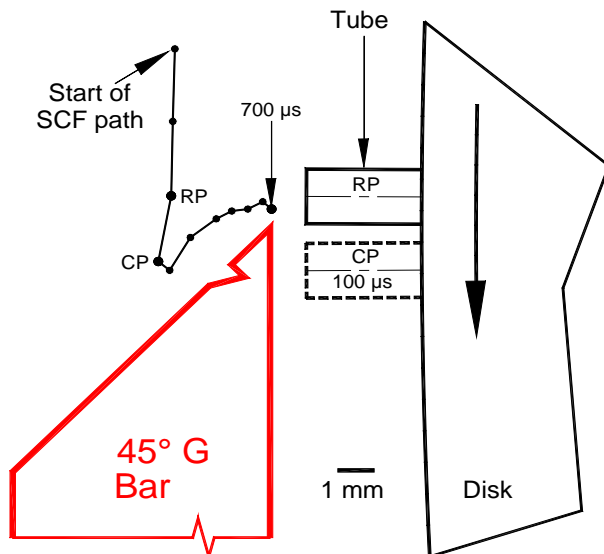


Figure 10. Grid bar: 45° G. The distance from the toe to the 2nd corner is 1.5 mm (0.059 in). The SCF was not removed.

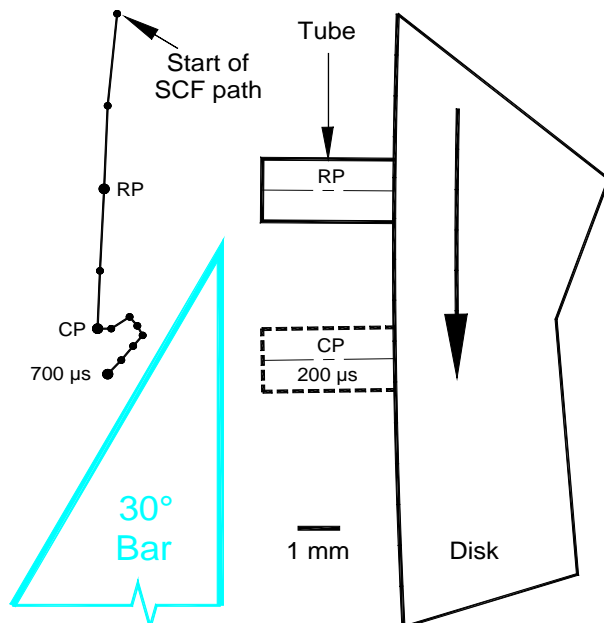


Figure 11. Grid bar: 30°. The distance from the toe to the 2nd corner is 14.9 mm (0.587 in). The SCF was removed at the toe of the grid bar.

Figure 9 shows the results of the SCF colliding with the 45° grid bar. At CP, the fiber bundle was wrapped around the leading (and only) edge of the grid bar, but the fiber bundle never pulled the SCF back towards the disk. This indicates that the grid bar, and not the fiber bundle, was most influential in removing the SCF. At CP, the velocity of the SCF in the y-direction was -16.5 m/s (-54.1 ft/s, Table 2). After the SCF was removed, it traveled in a mostly horizontal direction away from the disk. The velocity of the SCF in the x- and y-direction 700 μ s after impact was -2.41 and 0.86 m/s (-7.91 and 2.82 ft/s, Table 3), respectively.

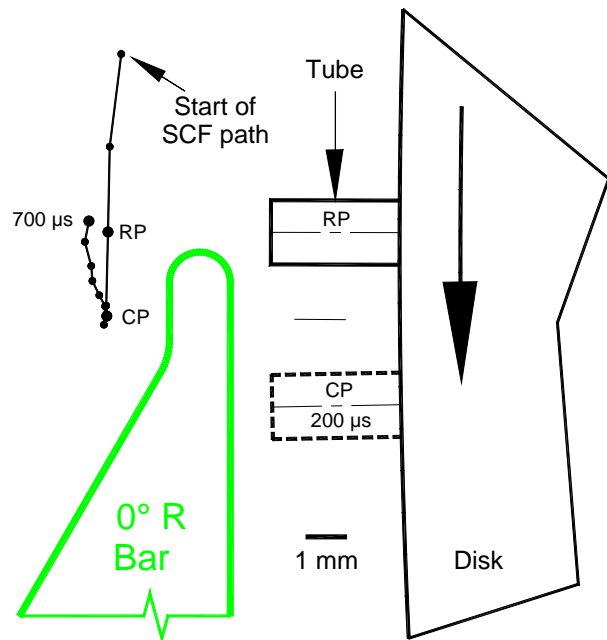


Figure 12. Grid bar: 0° R. The arc length is 2.36 mm (0.093 in). The SCF was removed around the radius of the grid bar.

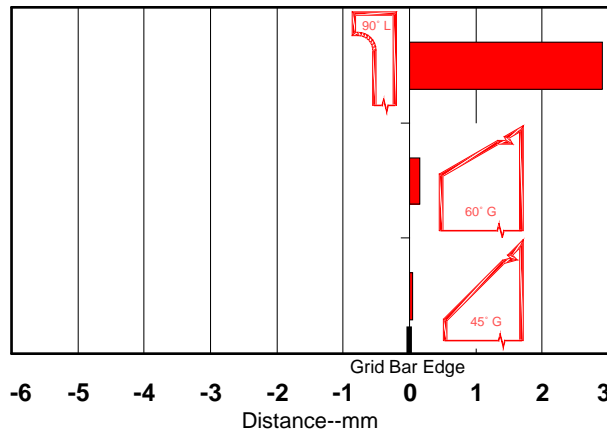


Figure 13. The position of the SCF in the x-direction 700 μ s after colliding with the 90° L, 60° G, and 45° G grid bars. Positive values indicate travel towards the disk (or lint cleaner saw), an undesirable situation.

Figure 10 shows the results of the SCF colliding with the 45° G grid bar. The results are similar to that of the 60° G grid bar: the fiber bundle continued to pull the SCF back towards the disk as it stretched over the grid bar; the groove did not function as a second edge to help remove the SCF because the groove was not large enough for the SCF to fit into, and the groove may have cushioned the impact of the SCF; and at 700 μ s after collision, the SCF was located between the grid bar and disk.

Figure 11 shows the results of the SCF colliding with the 30° grid bar. At CP, the fiber bundle was

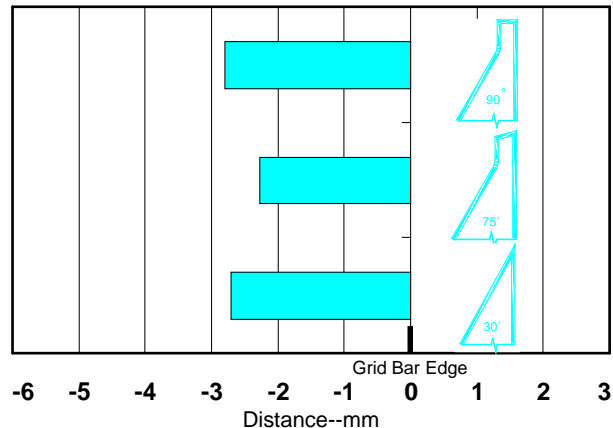


Figure 14. The position of the SCF in the x-direction 700 μ s after colliding with the 90°, 75°, and 30° grid bars. Negative values indicate travel away from the disk (a desirable situation).

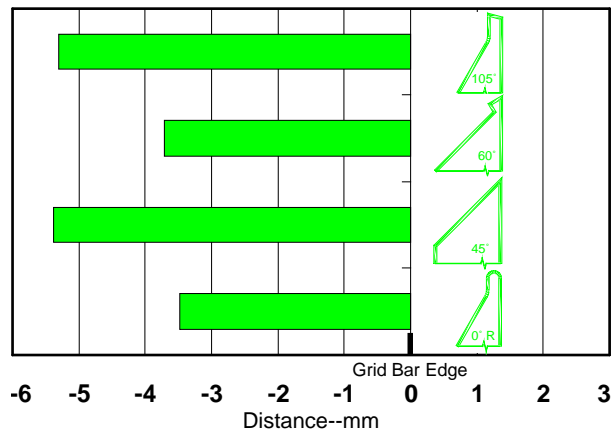


Figure 15. The position of the SCF in the x-direction 700 μ s after colliding with the 105°, 60°, 45°, and 0° R grid bars. Negative values indicate travel away from the disk (a desirable situation).

wrapped around the leading (and only) edge of the grid bar, and the SCF was removed at CP with little interaction from the bundle. After being removed from the fiber bundle, the SCF appeared to ricochet off of the grid bar and act as a free body in the downward direction, but remain close to the grid bar. The velocity of the SCF in the x- and y-direction 700 μ s after impact was -3.27 and -3.57 m/s (-10.7 and -11.7 ft/s, Table 3), respectively, and the SCF remained close to the grid bar.

Figure 12 shows the results of the SCF colliding with the 0° R grid bar. The 0° R grid bar did not have a sharp edge like the other nine grid bars in the experiment. At CP, the fiber bundle was wrapped around the radius of the grid bar. The SCF was removed from the fiber bundle shortly after colliding with the grid bar. At CP, the SCF had the lowest

velocity in the y-direction among all grid bars at -2.56 m/s (-8.40 ft/s, Table 2). The SCF traveled a short distance downward in the y-direction, and then turned around and traveled upward away from the grid bar. The velocity of the SCF in the x- and y-direction 700 μ s after collision was 0.99 and 5.13 m/s (3.25 and 16.8 ft/s, Table 3). It is interesting that the rounded grid bar removed the SCF, especially because the grid bar resembled a dull standard grid bar. Although the SCF was removed, it might take longer to be deposited with the trash because it traveled in a mostly upward direction.

As mentioned earlier, SCF traveling in a horizontal direction away from the disk was the most desirable situation because the SCF would be removed from the fiber bundle still attached to the disk, and theoretically the SCF would be collected with the trash. Using the distance traveled in the x-direction after impact with the grid bar aided in choosing which grid bars to build and test on a full-size lint cleaner. Figures 13, 14, and 15 show the horizontal position of the SCF, relative to the leading edge of the grid bar, 700 μ s after colliding with the grid bars (the first column in Table 3). Figure 13 shows undesirable situations where the horizontal position of the SCF 700 μ s after impact with the grid bar was on the disk-side of the grid bar edge. The SCF position was 2.9, 0.16, and 0.04 mm (0.114, 0.006, and 0.002 in) on the disk-side of the grid bar edge after impacting the 90° L, 60° G, and 45° G grid bar, respectively; the SCF was not removed from the fiber bundle. As mentioned earlier, the 60° G and 45° G grid bars had a 0.51-mm (0.020-in) deep groove on the surface of the bar approximately 1.5 mm (0.059 in) from the toe of the bar. The groove did not function as a second edge to help remove the SCF because the groove was not large enough for the SCF to fit into, and the groove might have cushioned the impact of the SCF. All three grid bars shown in Fig. 13 were considered to be inferior designs because they did not remove the SCF.

Figure 14 shows situations where the horizontal position of the SCF 700 μ s after impact with the grid bar was a short distance away (negative on x-coordinate) from the grid bar edge and disk. The SCF position was -2.79, -2.28, and -2.71 mm (-0.110, -0.091, and -0.106 in) away from the grid bar edge after impacting the 90°, 75°, and 30° grid bar, respectively, and the SCF was removed from the fiber bundle with all three grid bar designs. The grid bars shown in Fig. 14 were considered to be

adequate designs because they did remove the SCF, but the SCF did not travel away from the disk as far as others grid bars in the experiment.

Figure 15 shows situations where the SCF traveled the farthest distance away from the grid bar edge and disk 700 μ s after impact with the grid bars. The SCF position was -5.3, -3.7, -5.4, and -3.5 mm (-0.209, -0.146, -0.213, and -0.138 in) away from the grid bar edge after impacting the 105°, 60°, 45°, and 30° grid bar, respectively, and the SCF was removed from the fiber bundle with all four grid bar designs. Although the 0° R grid bar resembled a dull standard grid bar, it was effective in removing a SCF. The grid bars shown in Fig. 15 were considered to be superior designs because they did remove the SCF, and interaction with the grid bar caused the SCF to travel the farthest distance away from the grid bar edge 700 μ s after impact with the grid bar.

SUMMARY AND CONCLUSIONS

A 60-lot experiment examined the action of an SCF colliding with 10 different experimental grid bars mounted on a lint cleaner simulator. Results showed that grid bars that had an included angle of the sharp toe of the grid bar larger than the included angle found on conventional grid bars appeared to adequately remove a SCF, and grid bars that had a second corner a short distance from the toe of the grid bar appeared to remove the SCF from the fiber bundle more quickly and completely. It appeared that if the SCF made a fast and clean break away from the fiber bundle, the SCF retained more energy and its momentum continued for a longer time period. Conversely, it appeared if fibers were slowly pulled off of the SCF (not a clean break), then the energy of the SCF was dissipated, and the momentum of the SCF was reduced. It was found that embedding a small groove onto the impact surface of an experimental grid bar was less effective in removing the SCF. Although there was a considerable amount of variability in the data, the three replications run were sufficient to find statistically significant differences in several of the grid bar designs. Considering the position of the SCF a short time (700 μ s) after impact with the grid bar, the grid bars that had a 105°, 60°, and 45° included angle from the toe of the grid bar, and the rounded grid bar with about a 0.76-mm (0.030-in) radius, performed best in removing a SCF from the fiber bundle. These grid bar designs warrant further testing on a full-size conventional saw-type lint cleaner.

ACKNOWLEDGMENT

The authors would like to thank Cotton Incorporated, Cary, NC, for their assistance on this research.

DISCLAIMER

Mention of trade names or commercial products in this publication is solely for the purpose of providing specific information and does not imply recommendation or endorsement by the U.S. Department of Agriculture.

REFERENCES

- Armijo, C.B., S.E. Hughs, M.N. Gillum, and E.M. Barnes. 2006a. Ginning a cotton with a fragile seed coat. *J. Cotton Sci.* 10:46–52.
- Armijo, C.B., G.A. Holt, K.D. Baker, S.E. Hughs, E.M. Barnes, and M.N. Gillum. 2006b. Harvesting and ginning a cotton with a fragile seed coat. *J. Cotton Sci.* 10:311–318.
- Armijo, C.B., D.P. Whitelock, E.M. Barnes, and M.N. Gillum. 2008. Innovative technique to evaluate lint cleaner grid bar designs. p. 672–680. *In Proc. Beltwide Cotton Conf.*, Nashville, TN. 8-11 Jan. 2008. Natl. Cotton Counc. Am., Memphis, TN.
- Armijo, C.B., K.D. Baker, S.E. Hughs, E.M. Barnes, and M.N. Gillum. 2009a. Harvesting and seed cotton cleaning of a cotton cultivar with a fragile seed coat. *J. Cotton Sci.* 13:158–165.
- Armijo, C.B., D.P. Whitelock, S.E. Hughs, E.M. Barnes, and M.N. Gillum. 2009b. Diagramming the path of a seed coat fragment on experimental lint cleaner grid bars. p. 521–530. *In Proc. Beltwide Cotton Conf.*, San Antonio, TX. 5-8 Jan. 2009. Natl. Cotton Counc. Am., Memphis, TN.
- Baker, R.V., and A.D. Brashears. 1989. Effects of grid and saw variables on lint cleaner performance. *Trans. of ASAE* 32:1138–1142.
- Leonard, C.G., T.E. Wright, and S.E. Hughs. 1982. Lint cotton cleaners with notched grid bars. *Trans. of ASAE* 25:204–209.
- Mangialardi, G.J. 1987. Relationship of lint cleaning to seed coat fragments. p. 535–536. *In Proc. Beltwide Cotton Prod. Res. Conf.*, Dallas, TX. 4-8 Jan. 1987. Natl. Cotton Counc. Am., Memphis, TN.
- Mangialardi, G.J., and J.V. Shepherd. 1968. Seed coat fragment and funiculus distribution in ginned lint as affected by lint cleaning. ARS Report 42-145, June 1968. USDA, ARS, Beltsville, MD.
- Ray, S.A. 2006. Alternative configurations in a cylinder-type cleaner for seed cotton. *Appl. Eng. Agric.* 22:643–649.
- Wanjura, J.D., G.A. Holt, and J.A. Carroll. 2009. Influence of grid bar shape on field cleaning performance – screening tests. p. 439–448. *In Proc. Beltwide Cotton Conf.*, San Antonio, TX. 5-8 Jan. 2009. Natl. Cotton Council Am., Memphis, TN.
- Whitelock, D.P., and W.S. Anthony. 2003. Evaluation of cylinder cleaner grid bar configuration and cylinder speed for cleaning of seed cotton, lint, and lint cleaner waste. *Appl. Eng. Agric.* 19:31–37.